

On the nonlinearity of the Langmuir turbulence excited by a weak electron beam-plasma interaction

Y. Nariyuki¹ and T. Umeda²

¹Department of Electrical Engineering and Information Science, Kochi National College of Technology, Kochi 783-8508, Japan

²Solar-Terrestrial Environment Laboratory, Nagoya University, Nagoya, Aichi 464-8601, Japan

(Received 15 February 2010; accepted 15 April 2010; published online 18 May 2010)

In the present study, we analyze the data sets produced by a one-dimensional Vlasov–Poisson simulation of the weak electron beam-plasma instability to clarify the nonlinearity of the Langmuir turbulence excited by the weak-beam interaction. The growth of wave number modes is analyzed by using the momentum equation of the whole electrons. The analysis shows that the primary Langmuir wave mode is almost linear, while the nonlinear terms play important roles in the growth of the lower harmonic mode and the secondary higher harmonic mode. After the linear growth saturates, while the wave power of the primary mode is much larger than the other modes, linear and nonlinear interactions occurring in both lower harmonic and secondary higher harmonic modes are more active than those in the primary mode. Nonlinearity in the system comes from the advection rather than the ponderomotive forces. © 2010 American Institute of Physics. [doi:10.1063/1.3425872]

The amplitude-modulated Langmuir waves are frequently observed in space plasmas.^{1–3} The past numerical studies have suggested that some of the Langmuir turbulence in space plasmas and in type III solar radio bursts are consequences of electron beam-plasma instabilities.^{4–8,12,10} In the case of weak electron beam-plasma interactions, the mechanism of the amplitude modulation is thought to be due to the nonlinear trapping of beam electrons by excited Langmuir waves.^{5,6}

On the other hand, the previous Vlasov simulations of a weak electron beam-plasma interaction have shown that Langmuir waves are not directly modulated by the nonlinear trapping but are modulated by the nonlinear interaction between the most unstable primary Langmuir mode and its sideband modes.^{8–10} Silin *et al.*¹⁰ has suggested that the temporal change of velocity distribution function (VDF) of beam electrons due to the nonlinear trapping and the plateau formation lead to a broadband wave number spectrum, which corresponds to the envelope modulation in the real space, due to higher wave number shift of the linearly unstable modes.

The purpose of this Brief Communication is to clarify the nonlinearity of the Langmuir turbulence excited by the weak-beam interaction. We analyze the data sets produced by a one-dimensional Vlasov–Poisson simulation of the weak electron beam-plasma instability with the same parameters as Silin *et al.*¹⁰

We adopt the “splitting method”¹¹ and the positive interpolation for hyperbolic conservation laws scheme¹² suggested for time advancement of the one-dimensional electrostatic Vlasov equation,

$$\frac{\partial f_e}{\partial t} + v_x \frac{\partial f_e}{\partial x} - \frac{eE_x}{m_e} \frac{\partial f_e}{\partial v_x} = 0, \quad (1)$$

where f_e is the VDF of electrons, m_e is the electron mass, and e is the elementary electric charge, v_x and E_x are the

velocity and electric field along the simulation domain (x), respectively. In our run, two electron components, which are a very weak electron beam and background major electrons, are initially given with the same plasma parameters as the previous study.¹⁰ The beam and background electrons have the equal thermal velocity $v_{th} = \sqrt{(k_B T_e)/m_e} = 0.125v_d$, where k_B is the Boltzmann factor, T_e is the electron temperature, and $v_d (=1)$ is the beam drift velocity, respectively. The density ratio of the beam component is $R = n_b/(n_c + n_b) \sim 0.003$, where the subscripts c and b represent background core electrons and beam electrons, respectively. The total electron plasma frequency ω_e , m_e , $n_e (=n_c + n_b)$, and e are also assumed to be unity. Since ion dynamics is negligible for the evolution of the system with the above parameters, as shown in the previous study,¹⁰ we consider ions as an immobile background in the present study. The simulation domain is taken along an ambient magnetic field. We use periodic boundary conditions in the real space, and open boundary conditions in the velocity space. The number of cells is $N_x = 2048$ in the x direction and is $N_{v_x} = 400$ in the v_x direction over a velocity range from $v_{max} = 1.5v_d$ to $v_{min} = -1.5v_d$. The grid spacing is $\Delta x = 0.25v_d/\omega_e = 0.03125v_{th}/\omega_e$, and the time step is $\Delta t = 0.02/\omega_e$. We initially impose a seed density perturbation $\delta n_e \sim \pm 10^{-10}$ as a white noise.¹³

Silin *et al.*¹⁰ modeled the nonlinear deformations of the VDFs by using a simple analytic function, which represent the transition from the initial VDFs [$s=1$ in Eq. (2)] to the stationary Maxwellian with a flat shoulder [$s=6$ in Eq. (2)] as follows:¹⁰

$$k^2 = \frac{(1-R)}{2v_{th}^2} Z'(z_e) + \frac{1}{s} \sum_{n=1}^s \frac{R}{2v_{th}^2} Z'(z_{bn}), \quad (2)$$

where Z is the plasma dispersion function, $Z'(z_*) = -2[1 + z_* Z(z_*)]$, $z_e = \omega/(\sqrt{2}kv_{th})$, and $z_{bn} = \{\omega + [v_d - (n-1)v_{th}]k\}/(\sqrt{2}kv_{th})$.

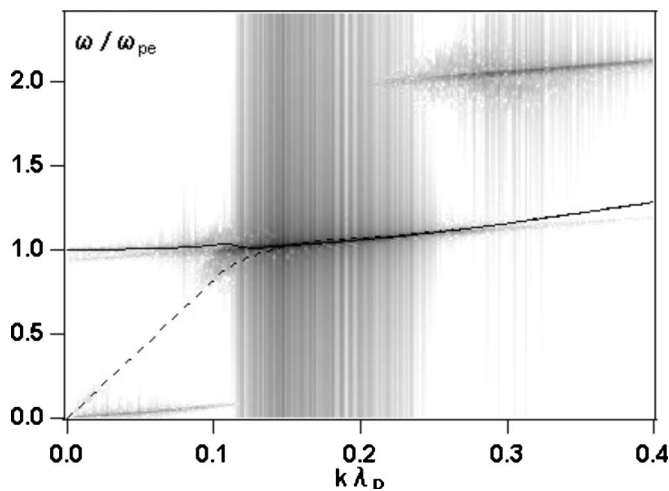


FIG. 1. The ω - k spectrum of the electric field (E_x) on a logarithmic scale, and the linear dispersion relation with the initial VDFs (dashed line) and with the stationary Maxwellian with a flat shoulder (solid line).

In the present study, we reperform the numerical simulation with the same parameters as the run in Silin *et al.*,¹⁰ and make more detailed analysis in terms of nonlinearity. However, before analyzing the numerical simulation result, let us revisit the linear theory of Silin *et al.*,¹⁰ since we have two queries in their analysis: one is about the linear dispersion relation itself, and another is about comparison between the linear dispersion relation and the ω - k spectrum observed in their simulation.

The former is that a straight line corresponding to the electron beam mode ($\omega = v_d k$) seems to appear [Fig. 9(a) in Ref. 10], even when the VDF is a stationary Maxwellian with a flat shoulder in spite of the beam electrons [$s=6$ in Eq. (2)] used. Electron beam instabilities should not appear after flat shoulder is formed. Thus we expect that there may be some errors or miscalculations of the dispersion relation in their analysis.¹⁰ In their equations, it seems that the differences lie in the definition of the thermal velocity used in the plasma dispersion function.^{14,15} Actually, by numerically solving Eq. (2) with the correct definition of v_{th} ($=\sqrt{(k_B T_e)/m_e}$) and z_s , the plasma oscillationlike blanch appears in the stationary Maxwellian with the flat shoulder (the solid line in Fig. 1).

The latter is that after the linear instability saturates [Fig. 10(d) in Ref. 10], the numerical ω - k spectrum at $k\lambda_{De} > 0.2$ (λ_{De} is the Debye length) is not along the linear dispersion relation, but shows a straight line, whose slope possibly corresponds to the group velocity of Langmuir wave packets due to the nonlinear wave-wave interactions, however there is no explanation to this in Silin *et al.*¹⁰ It may also be due to the issues mentioned above: the present linear analysis agrees better with the numerical dispersion relation of the primary Langmuir wave mode ($\omega \sim \omega_e$) than that in Silin *et al.*¹⁰ (Fig. 1), while the nonlinear wave-wave interaction in the primary wave mode is weak as will be shown later. In summary, we believe there are some errors or miscalculations of the dispersion relation in Silin *et al.*,¹⁰ although these errors do not influence their conclusions themselves.

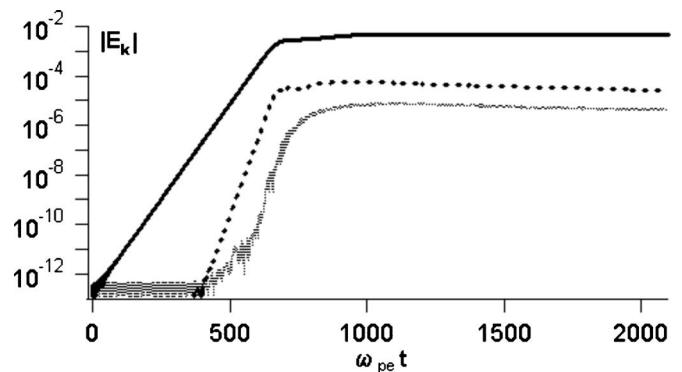


FIG. 2. Time evolution of the wave number spectrum with $k\lambda_{De}=0.1488$ (solid line), $k\lambda_{De}=0.2976$ (bold dashed line), and $k\lambda_{De}=0.03$ (gray line), respectively.

Figure 1, which is the secondary higher harmonic mode ($\omega \sim 2\omega_e$), is also excited at around $0.25 < k\lambda_{De} < 0.32$. As shown in the past theoretical and numerical studies,^{13,16} these higher harmonic modes are linearly excited (the bold dashed line in Fig. 2). In addition, the lower harmonic mode is also excited around $0 < k\lambda_{De} < 0.1$, which does not appear in the quasilinear theory,¹⁶ since their growth is nonlinear (the gray line Fig. 2).

We will next discuss the growth of these three modes (primary mode, higher harmonic modes, and lower harmonic mode) by using the momentum equation of the whole electrons,

$$\frac{\partial j_x}{\partial t} = -\frac{\partial j_x u_x}{\partial x} + \frac{e}{m_e} \rho_e E_x + \frac{e}{m_e} \frac{\partial p_e}{\partial x}, \quad (3)$$

where j_x , u_x , ρ_e , and p_e are the total parallel current, the total parallel bulk velocity, the total electron charge density, and the total electron pressure, respectively. We note that Eq. (3) is exactly derived from Eq. (1), which includes both background and beam electrons. Assuming $e/m_e=1$ and rewriting the second term of the right hand side (RHS) of Eq. (3) using Gauss's law, we have

$$\frac{\partial j_x}{\partial t} = -\frac{\partial j_x u_x}{\partial x} + E_x - \frac{1}{2} \frac{\partial E_x^2}{\partial x} + \frac{\partial p_e}{\partial x}, \quad (4)$$

where the first, second, third, and fourth terms of RHS are the nonlinear terms due to the advection, the linear term indicating the plasma oscillation, the nonlinear term due to the ponderomotive force, and the linear term due to the plasma pressure gradient, respectively. We note that the nonlinear terms of RHS are negligible and the fourth term behaves like the growth term at the linear stage, since the initial uniform j_x and u_x are quite small ($\sim 10^{-10}$), due to the small population of the beam components. By calculating each term of RHS in Eq. (3), we can directly evaluate the linear and nonlinear instabilities. To discuss the growth of primary mode, higher harmonic modes, and lower harmonic mode, we examine each term of the RHS in Eq. (4) in the Fourier space. We write the Fourier transformed variables with the wave number k as $g_k = |g_k| \exp i\phi_k^g$, where $g = j_x, E_x, u_x, p_e$, and $P_x = \frac{1}{2} E_x^2$. Hereafter, the subscripts of x and e are neglected in

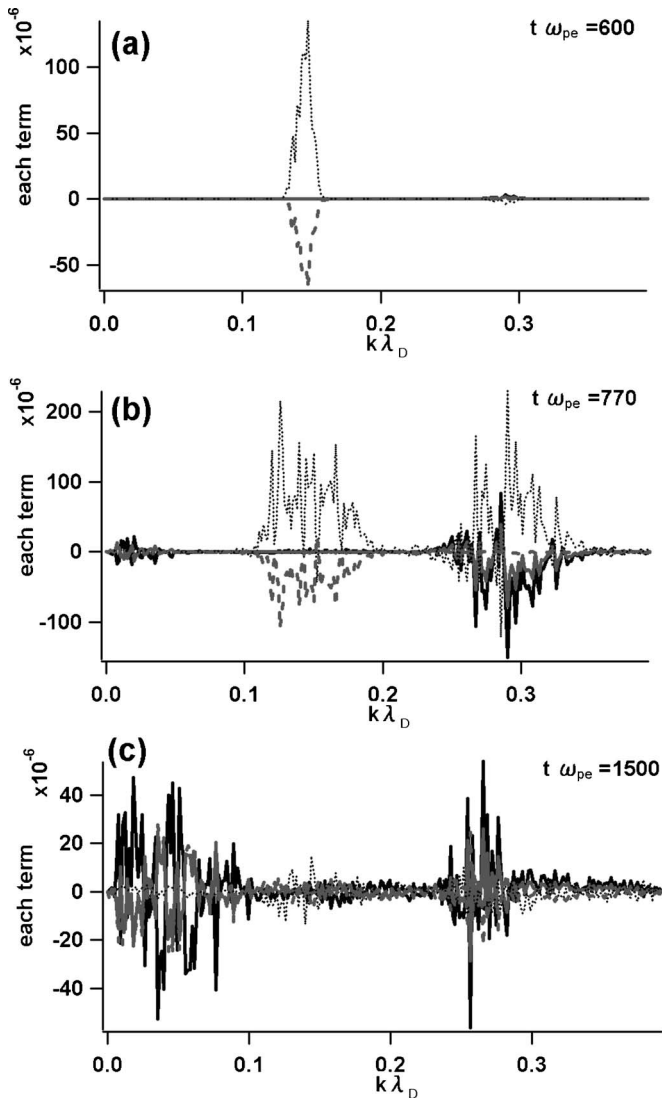


FIG. 3. F_{adv} (black solid line), F_{osc} (gray dashed line), F_{pon} (gray solid line), and F_{prs} (black dotted line) at (a) $t\omega_e=600$, (b) $t\omega_e=770$, and (c) $t\omega_e=1500$, respectively.

the Fourier transformed variables. By Fourier transforming Eq. (4), we obtain

$$\frac{d|j_k|}{dt} = F_{tot} = F_{adv} + F_{osc} + F_{pon} + F_{prs},$$

where

$$F_{adv} = k \sum_{k=k_1+k_2} |j_{k_1}| |u_{k_2}| \sin(\theta_{k=k_1+k_2}^{ju}),$$

$$F_{osc} = |E_k| \cos(\theta_k^E),$$

$$F_{pon} = k |P_k| \sin(\theta_k^P),$$

$$F_{prs} = -k |P_k| \sin(\theta_k^P),$$

$$\theta_{k=k_1+k_2}^{ju} = \phi_k^j - \phi_{k_1}^j - \phi_{k_2}^u,$$

and

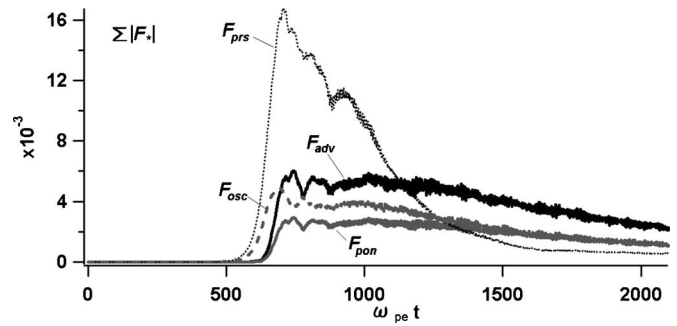


FIG. 4. $\sum_{k=0}^{k_{max}} |F_*|$ where $k_{max} = \pi\omega_e/v_d$. What each line indicates is same as Fig. 3.

$$\theta_k^{g1g2} = \phi_k^{g1} - \phi_k^{g2}.$$

Figure 3 shows the F_* at (a) $t\omega_e=600$, (b) $t\omega_e=770$, and (c) $t\omega_e=1500$, respectively. As shown in Fig. 3(a), the growth of the primary Langmuir mode due to F_{prs} and F_{osc} is dominant at the linear stage. After the modes with the maximum growth rate saturates, the growth of the other primary wave modes ($0.1 < k\lambda_{De} < 0.2$) and the secondary higher harmonic mode ($0.25 < k\lambda_{De} < 0.32$) is enhanced [Fig. 3(b)]. We note that the nonlinear terms (F_{adv} and F_{pon}) are more active than the linear term F_{osc} for the secondary higher harmonic mode, while F_* for the lower harmonic wave modes ($k\lambda_{De} < 0.1$) is weaker at the same time. As time elapses, F_{prs} becomes smaller but broader in a wide wave number range of the primary and the secondary higher harmonic mode, while the lower harmonic mode begins to grow due to the nonlinear terms.

After the linear growth saturates, F_* for the primary mode is small, while those for the lower harmonic mode and the secondary higher harmonic mode remain active [Fig. 3(c)]. Namely, while the power of the primary mode is much larger than the other modes (Fig. 2), linear and nonlinear interactions in the primary mode are much smaller than those in the other modes. Moreover, $|F_{adv}|$ is larger than $|F_{pon}|$ in both lower and higher harmonic modes. $|F_{pon}|$ is very similar to $|F_{prs}|$ at $t\omega_e=1500$.

Figure 4 shows $\sum_{k=0}^{k_{max}} |F_*|$, where $k_{max} = \pi\omega_e/v_d$. Time evolution of the total amount of each F_* clearly shows the characteristics described above. Nonlinear interactions (F_{adv} and F_{pon}) among Fourier modes play more important roles in evolution of the system than the linear interactions after $t\omega_e \sim 1100$.

To conclude, we revisit the evolution process of the Langmuir turbulence excited by the weak-beam interaction. The present analysis shows that the primary mode is almost linear, which is in agreement with Silin *et al.*,¹⁰ while the lower harmonic mode and the secondary higher harmonic mode are nonlinear after the linear growth saturates. Moreover, nonlinearity in the system comes from the advection (F_{adv}) rather than the ponderomotive forces (F_{pon}). This result suggests that the Langmuir turbulence excited by weak-beam instability is not consistent with one in Zakharov systems.^{17,18}

This work was supported by Grant-in-Aid for Young Scientists (Start-up) (Grant No. 20840042) from JSPS, and Grant-in-Aid for Young Scientists (B) (Grant No. 21740352) (T.U.) and (Grant No. 22740324) (Y.N.) from MEXT of Japan.

- ¹D. A. Gurnett, G. V. Hospodarsky, W. S. Kurth, D. J. Williams, and S. J. Bolton, *J. Geophys. Res.* **98**, 5631, doi:10.1029/92JA02838 (1993).
- ²K. Stasiewicz, B. Holback, V. Krasnoselskikh, M. Boehm, R. Bostrom, and P. M. Kintner, *J. Geophys. Res.* **101**, 21515, doi:10.1029/96JA01747 (1996).
- ³J. Soucek, V. Krasnoselskikh, T. Dudok de Wit, J. Pickett, and C. Kletzing, *J. Geophys. Res.* **110**, A08102, doi:10.1029/2004JA010977 (2005).
- ⁴Y. Kasaba, Y. Omura, and H. Matsumoto, *J. Geophys. Res.* **106**, 18693, doi:10.1029/2000JA000329 (2001).
- ⁵K. Akimoto, Y. Omura, and H. Matsumoto, *Phys. Plasmas* **3**, 2559 (1996).
- ⁶H. Usui, H. Furuya, H. Kojima, H. Matsumoto, and Y. Omura, *J. Geophys. Res.* **110**, A06203, doi:10.1029/2004JA010703 (2005).
- ⁷T. Umeda, *J. Geophys. Res.* **115**, A01204, doi:10.1029/2009JA014643 (2010).
- ⁸T. Umeda, *Phys. Plasmas* **13**, 092304 (2006).
- ⁹T. Umeda, *Nonlinear Processes Geophys.* **14**, 671 (2007).
- ¹⁰I. Silin, R. Sydora, and K. Sauera, *Phys. Plasmas* **14**, 012106 (2007).
- ¹¹C. Z. Cheng and G. Knorr, *J. Comput. Phys.* **22**, 330 (1976).
- ¹²T. Umeda, *Earth, Planets Space* **60**, 773 (2008).
- ¹³T. Umeda, Y. Omura, P. H. Yoon, R. Gaelzera, and H. Matsumoto, *Phys. Plasmas* **10**, 382 (2003).
- ¹⁴T. H. Stix, *Waves in Plasmas* (American Institute of Physics, New York, 1992), pp. 199–206.
- ¹⁵S. P. Gary, *Theory of Space Plasma Microinstability* (Cambridge University Press, 1993), pp. 30–33.
- ¹⁶P. H. Yoon, R. Gaelzera, T. Umeda, Y. Omura, and H. Matsumoto, *Phys. Plasmas* **10**, 364 (2003).
- ¹⁷P. A. Robinson, *Rev. Mod. Phys.* **69**, 507 (1997).
- ¹⁸J. Soucek, T. Dudok de Wit, V. Krasnoselskikh, and A. Volokitin, *Ann. Geophys.* **21**, 681 (2003).